

Incommensurate magnetic ordering in $\text{Cu}_2\text{Te}_2\text{O}_5\text{X}_2$ ($\text{X} = \text{Cl}, \text{Br}$) studied by single crystal neutron diffraction

O. Zaharko, H. Rønnow, J. Mesot

Laboratory for Neutron Scattering, ETHZ & PSI, CH-5232 Villigen, Switzerland

S. J. Crowe, D. McK. Paul

Department of Physics, University of Warwick, Coventry, CV4 7AL, United Kingdom

P. J. Brown

Institut Laue-Langevin, 156X, 38042 Grenoble Cedex, France

A. Daoud-Aladine

ISIS Facility, Rutherford Appleton Laboratory, Chilton,
Didcot, Oxfordshire OX10 0QX, United Kingdom

A. Meents, A. Wagner

Paul Scherrer Institute, CH-5232 Villigen, Switzerland

M. Prester

Institute of Physics, P.O.B. 304, HR-10 000, Zagreb, Croatia

H. Berger

Institut de Physique de la Matière Complexe, EPFL, CH-1015 Lausanne, Switzerland

(dated: March 23, 2024)

Polarized and unpolarized neutron diffraction studies have been carried out on single crystals of the coupled spin tetrahedra systems $\text{Cu}_2\text{Te}_2\text{O}_5\text{X}_2$ ($\text{X} = \text{Cl}, \text{Br}$). A model of the magnetic structure associated with the propagation vectors $\mathbf{k}_{\text{Cl}}^0 = (0.150; 0.422; \frac{1}{2})$ and $\mathbf{k}_{\text{Br}}^0 = (0.172; 0.356; \frac{1}{2})$ and stable below $T_N = 18 \text{ K}$ for $\text{X} = \text{Cl}$ and $T_N = 11 \text{ K}$ for $\text{X} = \text{Br}$ is proposed. A feature of the model, common to both the bromide and chloride, is a canted coplanar motif for the 4 Cu^{2+} spins on each tetrahedron which rotates on a helix from cell to cell following the propagation vector. The Cu^{2+} magnetic moment determined for $\text{X} = \text{Br}$, $0.395(5) \mu_B$, is significantly less than for $\text{X} = \text{Cl}$, $0.88(1) \mu_B$ at 2 K . The magnetic structure of the chloride associated with the wave-vector \mathbf{k}^0 differs from that determined previously for the wave vector $\mathbf{k} = (0.150; 0.422; \frac{1}{2})$ [O. Zaharko, et al., Phys. Rev. Lett. 93, 217206 (2004)].

PACS numbers: 75.30.-m, 75.10.Jm, 61.12.Ld

I. INTRODUCTION

Systems with weakly interacting frustrated magnetic clusters form an interesting class of materials with properties lying between those of quantum spin systems and classical magnets.¹ In this context the $\text{Cu}_2\text{Te}_2\text{O}_5\text{X}_2$ ($\text{X} = \text{Cl}, \text{Br}$)² compounds have recently attracted strong interest, as they contain Cu^{2+} tetrahedral clusters. The antiferromagnetic exchange interactions between the spins within a tetrahedron are geometrically frustrated and the coupling between the tetrahedra was assumed to be weak. Whilst the excitation spectrum of isolated tetrahedra is well known to be gapped, the presence of even small anisotropy or inter-tetrahedral coupling may lead to interesting new ground states and excitations. In these compounds the magnetic susceptibility reaches a maximum at $T \approx 25 \text{ K}$ before dropping sharply at low temperatures, which was attributed to the presence of a singlet-triplet spin-gap.^{2,3} Further evidence of spin-gapped behavior in the bromide is observed in Raman

scattering,^{3,4,5} which also reveals evidence of what is suggested to be a low energy longitudinal magnon. Fitting the susceptibility data to an isolated tetrahedral model with four nearest neighbour (J_1) and two next nearest neighbour (J_2) exchange interactions gives the coupling strengths $J_1 = J_2 = 43 \text{ K}$ and 38.5 K for $\text{X} = \text{Br}$ and Cl respectively. However, susceptibility,^{2,3} heat capacity^{3,5} and thermal conductivity^{6,7} measurements all show evidence of magnetic ordering at low temperatures, $T_N = 18 \text{ K}$ (Cl) and 11 K (Br), which requires inter-tetrahedral couplings. The effect of inter-tetrahedral coupling and the relative strengths of exchange interactions in this system have been investigated theoretically by band structure calculations,⁸ spin dimer analysis,⁹ low-equation method¹⁰ and a mean field analysis.^{4,5} The consequences of antisymmetric Dzyaloshinsky-Moriya (DM) interactions have been also analysed.¹¹ Experimentally, magnetic excitations with a dispersive component are observed in both compounds by inelastic neutron scattering measurements,^{12,13} which

are associated with the development of long range order. The ground state magnetic structure is found from neutron diffraction studies to be rather complex.¹⁴ Both compounds have incommensurate magnetic structures with wave-vectors $k_{C1}^0 = (0.150; 0.422; \frac{1}{2})$ and $k_{Br}^0 = (0.172; 0.356; \frac{1}{2})$. For $Cu_2Te_2O_5Cl_2$ the co-existence of two different magnetic structures with $k^0 = (k_x; k_y; \frac{1}{2})$ and $k = (k_x; k_y; \frac{1}{2})$ has been detected. In the model proposed for the k structure the four Cu^{2+} ions of each tetrahedron form two pairs with the spins on the two ions of a pair rotating in the same plane with a constant canting angle between them. The canting angles were determined as 38(6)° for the first and 111(10)° for the second pair.

II. NEW DIFFRACTION RESULTS

To obtain a more complete picture of the ground states of $Cu_2Te_2O_5X_2$ we have made several new diffraction experiments. An X-ray diffraction experiment was carried out on a $Cu_2Te_2O_5Cl_2$ single crystal (10 mm^3) at 10 K and 25 K at the X10 beam line ($\lambda = 0.71073\text{ Å}$) at the SLS synchrotron. It revealed that the crystal structure of $Cu_2Te_2O_5Cl_2$ at temperatures below and above T_N , has the same tetragonal space group $P\bar{4}$, as it does at 300 K.² The group is non-centrosymmetric and racemic twins were found to be present with the volume ratio 37(4):63(4). No features which could explain the co-existence of wave vectors k and k^0 below T_N were detected. The possibility of growth twins related by reflection in 100 planes was considered. No evidence for such twinning was obtained in the structure refinements confirming that the $fhklg$ and $f-khlg$ families of reflections are independent.

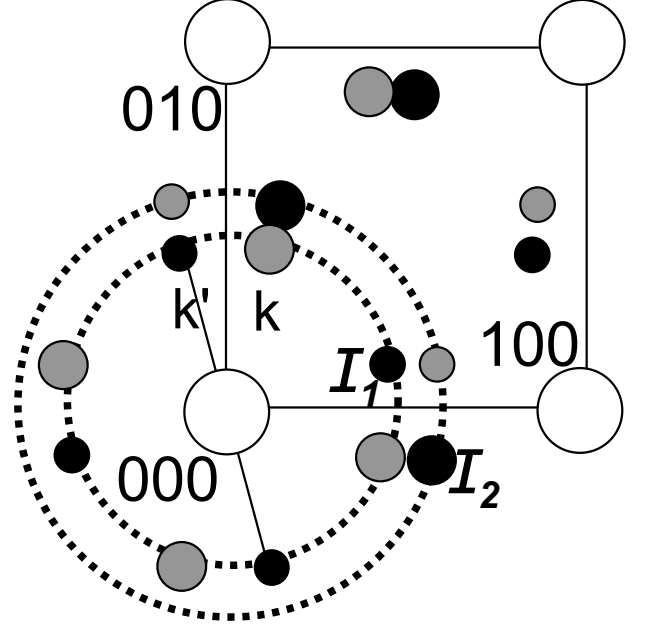
Spherical neutron polarimetric measurements were made at 2 K on a $Cu_2Te_2O_5Cl_2$ single crystal ($6 \times 2.8 \times 2.6\text{ mm}^3$) with CRYOPAD II installed on the D3 diffractometer at ILL ($\lambda = 0.843\text{ Å}$). These were supplemented by unpolarized integrated intensity measurements at 2 K on the same $Cu_2Te_2O_5Cl_2$ crystal and on a $Cu_2Te_2O_5Br_2$ ($4 \times 1 \times 1\text{ mm}^3$) crystal using the D10 diffractometer at ILL ($\lambda = 2.359\text{ Å}$).

The magnetic diffraction patterns given by the various $Cu_2Te_2O_5X_2$ crystals studied so far show an important qualitative difference. The $Cu_2Te_2O_5Cl_2$ crystal used in the present experiment gave 4 magnetic reflections at the lowest 2 θ value (black spots in Fig. 1). They originate from two conformation domains with wave vectors k^0 related by the four-fold axis (rotation of 90°). For the $Cu_2Te_2O_5Br_2$ crystal on the other hand only 2 reflections, corresponding to a single conformation domain, were found at the lowest angle (black spots connected by solid lines in Fig. 1). It should be recalled that in the previous study¹⁴ 8 reflections from two conformation domains of two independent wave vectors k^0 and k were reported (black and grey spots in Fig. 1).

There is a quantitative difference between the intensities of corresponding reflections obtained from the propagation vectors k and k^0 . This difference can be clearly seen by comparing the intensities I_1 and I_2 of the reflections $000 + k$ and $100 - k$. For the $Cu_2Te_2O_5Cl_2$ and $Cu_2Te_2O_5Br_2$ crystals studied in the present experiment the inequality $I_1 < I_2$ holds. In the previous study of another $Cu_2Te_2O_5Cl_2$ crystal¹⁴ this relation was the same $I_1 < I_2$ for the k^0 set, but opposite $I_1 > I_2$ for the k set; and it was from this latter set that the k structure was derived.¹⁵

In what follows we will describe the experimental observations made on wave vector k^0 and will use them to derive a model for the k^0 magnetic structure.

FIG. 1: The $hk0$ and $hk\frac{1}{2}$ layers of reciprocal space of a $Cu_2Te_2O_5X_2$ crystal. Black circles correspond to magnetic reflections $fhk\frac{1}{2}g$ of k^0 and grey circles - of k wave vectors. The circle radii are proportional to intensities of magnetic reflections. Dashed circles with center at 000 connect reflections with intensity I_1 and I_2 .



For polarimetric measurements the crystal was mounted with the a -direction vertical inside an ILL orange cryostat and cooled to 2 K. As the wave vector $k^0 = [0.150; 0.422; \frac{1}{2}]$ has a small a component, the beam scattered by a magnetic reflection hkl with $h = 0.15$ is tilted from the horizontal plane by an angle $\approx 1^\circ$ and can be measured by ensuring that the vertical aperture of the detector is wide enough. The inclination of the scattering vectors to the horizontal plane is $\approx 11.6^\circ$ for $k = 0.422; l = \frac{1}{2}$ and $\approx 4.6^\circ$ for $k = 0.422; l = \frac{3}{2}$. The polarization of the scattered beam was measured using a spin polarized 3He filter. The filter polarization decayed with a time constant of $\approx 100\text{ h}$ and its effective polar-

ization transmission varied from 0.73 to 0.55 between filter changes. The decay was followed by measuring the polarization scattered by the 002 nuclear reflection at regular intervals and an appropriate correction was applied to the scattered polarizations.

Measurements of each reflection were made with the incident neutrons polarized successively in three directions: parallel to the vertical z direction (P_z^0), along the x horizontal component of the scattering vector q (P_x^0) and in the y direction that completes the right-handed Cartesian set. In this polarization coordinate system the magnetic interaction vector ($M_\perp = C + iD$), which is the projection of the Fourier transform of the magnetization $M(r)$ onto the plane perpendicular to q , lies mainly in the yz -plane. For each incident polarization direction the components of scattered polarization parallel to the x , y and z directions were determined. The six magnetic reflections labelled h_1 - h_6 in Table I were studied. Their intensities were rather weak, and the background at low 2θ rather high, especially for the reflections h_1 ; h_2 ; h_3 , so reasonable statistics could only be obtained by measuring for about 6 hours/reflection. Even a qualitative analysis of the scattered polarization sets a number of valuable constraints on possible models for the magnetic structure of $\text{Cu}_2\text{Te}_2\text{O}_5\text{Cl}_2$.

The polarization P of neutrons scattered by a pure magnetic reflection can be written as:^{16,17}

$$PI = P^0(M_\perp \cdot M_\perp) + 2\langle M_\perp \cdot (P^0 \cdot M_\perp) \rangle \\ 2 = (M_\perp \cdot M_\perp) \quad (1)$$

with the first term parallel to P^0 , the second to M_\perp and the third to q . I is the scattered intensity which contains a polarization independent and a polarization dependent term:

$$I = M_\perp \cdot M_\perp + P^0 = (M_\perp \cdot M_\perp) \quad (2)$$

These equations rewritten in the form of polarization matrices:¹⁹

$$P_{ij} = \begin{matrix} \frac{M^2 + J_{yz}}{M^2 + J_{yz}} & 0 & 0 \\ \frac{J_{yz}}{M^2 + J_{yz}} & \frac{M^2 + R_{yy}}{M^2} & \frac{R_{yz}}{M^2} \\ \frac{J_{yz}}{M^2 + J_{yz}} & \frac{R_{yz}}{M^2} & \frac{M^2 + R_{zz}}{M^2} \end{matrix} \quad (3)$$

with $M^2 = M_\perp \cdot M_\perp$, $R_{ij} = 2R(M_\perp \cdot iM_\perp \cdot j)$ and $J_{ij} = 2J(M_\perp \cdot iM_\perp \cdot j)$ can be directly compared with the results presented in Table I.

Before attempting a detailed analysis, the different types of magnetic domains which can be present in $\text{Cu}_2\text{Te}_2\text{O}_5\text{X}_2$ should be considered. It is worth remembering¹³ that conformation, orientation and chiral magnetic domains are all possible. The conformation domains give rise to separate sets of magnetic peaks and are not important for the polarization data analysis. Orientation domains can occur if the z_x -axis is not

in the magnetic symmetry group. Chirality domains are present because the propagation vector k^0 is not one half of a reciprocal lattice vector ($k^0 \notin g \cdot k^0$). They are not the same as racemic twins which are allowed because the inversion center is missing in the crystallographic space group. The last two types of domain contribute to the same magnetic peaks and their presence could significantly complicate the D3 data analysis since orientation domains can depolarize the scattered beam and chirality domains can conceal the special features of helical structures.

It was found that within the statistical accuracy the scattered beam was fully polarized for all measured reflections which suggests that only one orientation domain is present. The two chiral domains are also unequally populated, since the h_1 and h_2 reflections were almost absent for incident polarization P_{+x}^0 , but had significant intensity for P_x^0 .

Furthermore, based on the polarization data we can immediately deduce the type of magnetic structure. The very presence of the x -components in the scattered polarization (P_{xy} and P_{xz}) indicates rotation of polarization towards q , which is not compatible with any amplitude modulated or collinear structure. Such structures would have $M_\perp \cdot kM_\perp$ and the neutron polarization would only precess by 180° about M_\perp . Therefore the magnetic structure must be helical.

The most significant qualitative conclusions from the polarimetric measurements are as follows:

1. The scattered polarization for the reflection h_2 with $q_2 \cdot k \cdot k^0$, shows that the structure is not composed of helices with spins rotating in a plane normal to the wave vector k^0 , for in such a case all polarization would be rotated towards the x direction. The presence of y and z components of scattered polarization indicates that one or more of the planes in which the spins rotate (plane of helices) must be inclined to the wave vector.
2. For all the reflections studied the P_{zz} components are positive, while P_{yy} are negative. i) This clearly indicates that all M_\perp vectors have a z -component, so there must be a component of the magnetic moment along a . ii) It also means that the z -components of M_\perp are larger than the y -components ($C_z^2 + D_z^2 > C_y^2 + D_y^2$). This might indicate that the planes of the helices are close to or contain the a -axis.
3. The magnitude of the P_{yy} and P_{zz} components tend to be larger for reflections with $l = \frac{3}{2}$ than for those with $l = \frac{1}{2}$ which strongly suggests the existence of a c -component of the magnetic moment.

Following the description of a magnetic structure given in reference,¹⁴ we express the moment S_{jl} of the j th Cu^{2+} ion in the l th unit cell as

$$S_{jl} = A_j \cos(k^0 \cdot r_{+j}) + B_j \sin(k^0 \cdot r_{+j}) \quad (4)$$

TABLE I: Polarization matrices P_{ij} measured for k^0 magnetic reflections of $\text{Cu}_2\text{Te}_2\text{O}_5\text{Cl}_2$ at 2 K (i-incoming, j-outcoming component of polarization). I is measured intensity.

h	k	l	P_i^0	P_{ix}	P_{iy}	P_{iz}	I
0.15 h_1	-0.42	$\frac{1}{2}$	-x	0.93(5)	-0.04(5)	0.19(4)	5.0(3)
			y	0.83(9)	-0.71(9)	0.03(8)	3.0(2)
			z	0.6(1)	-0.2(1)	1.0(1)	2.2(2)
			-z	1.2(1)	0.18(8)	-0.34(10)	2.2(2)
0.15 h_2	-0.42	$-\frac{1}{2}$	-x	0.93(8)	-0.03(9)	0.33(7)	4.5(2)
			y	0.8(2)	-0.5(2)	0.6(2)	2.7(1)
			z	0.7(2)	-0.0(2)	1.1(2)	2.3(1)
			-z	0.7(1)	-0.2(1)	-0.3(2)	3.1(4)
-0.15 h_3	-0.58	$\frac{1}{2}$	x	-1.03(3)	-0.04(3)	0.27(3)	6.4(1)
			y	-1.12(6)	-0.32(6)	-0.08(6)	3.6(1)
			z	-0.97(7)	-0.32(6)	0.55(6)	3.4(1)
-0.15 h_4	0.42	$\frac{3}{2}$	x	-0.88(10)	-0.11(8)	0.16(8)	2.3(1)
			-x	1.01(4)	0.06(4)	-0.16(4)	3.3(1)
			y	0.44(5)	-0.92(6)	-0.47(5)	3.9(1)
			z	0.56(5)	-0.40(4)	0.76(5)	3.8(4)
			-z	0.24(6)	0.32(5)	-0.88(5)	3.8(3)
-0.15 h_5	0.42	$-\frac{3}{2}$	x	-0.93(10)	0.03(8)	0.11(8)	2.0(3)
			y	0.52(6)	-0.73(6)	0.32(5)	3.0(4)
			z	0.54(6)	0.34(5)	0.88(6)	4.2(3)
0.15 h_6	-0.42	$\frac{3}{2}$	x	-0.92(6)	-0.10(6)	-0.27(4)	3.3(6)
			y	0.53(4)	-0.84(4)	-0.38(3)	4.4(1)
			z	0.43(4)	-0.61(3)	0.86(3)	3.4(2)

with r_l being the vector defining the origin of the l th unit cell. A_j and B_j are orthogonal vectors which determine the magnitude and direction of the helix associated with the j th ion, whilst ϕ_j defines its phase. The 4 independent Cu^{2+} moments of the $\text{Cu}_2\text{Te}_2\text{O}_5\text{Cl}_2$ unit cell could rotate on independent helices in which case it would be necessary to define the plane of each helix in polar coordinates by the angles θ_j, ϕ_j of B_j . There is freedom to choose the origin of each helix and a convenient choice is with the vector A_j in the ab plane ($\theta_j = 90^\circ$). For the class of models in which the four Cu^{2+} ions rotate as two canted pairs¹⁴ there are only two planes to define since the moments on the two ions of a pair rotate in the same one (θ, ϕ are the same). The difference between the values of the two ions is the canting angle for the pair, δ . Least-squares refinement of the θ, ϕ and δ parameters against the polarimetric measurements for the reflections h_1 - h_6 made using a CCL program¹⁸ lead to the following conclusions:

1. The data are sensitive to the difference between the angles of the two helices which defines the angle between the two planes, and to the absolute value of θ_B which defines their inclination to the c -axis. However, the sensitivity to the absolute values of the angle ϕ which defines their inclination to the

TABLE II: Polarization matrices P_{ij} calculated for a model of the k^0 magnetic structure of $\text{Cu}_2\text{Te}_2\text{O}_5\text{Cl}_2$ presented in Table III.

h	k	l	P_i^0	P_{ix}	P_{iy}	P_{iz}
0.15 h_1	-0.42	$\frac{1}{2}$	-x	0.97	0.00	0.26
			y	0.83	-0.53	0.15
			z	0.64	-0.02	0.77
			-z	0.97	0.02	-0.26
0.15 h_2	-0.42	$-\frac{1}{2}$	-x	0.97	0.00	0.26
			y	0.83	-0.53	0.19
			z	0.64	0.03	0.77
			-z	0.97	-0.02	-0.26
-0.15 h_3	-0.58	$\frac{1}{2}$	x	-0.94	-0.30	-0.13
			y	-0.98	-0.03	0.21
			z	-0.79	-0.34	0.50
-0.15 h_4	0.42	$\frac{3}{2}$	x	-0.98	-0.06	0.19
			-x	0.99	0.03	-0.13
			y	0.38	-0.80	-0.47
			z	0.54	-0.42	0.73
			-z	0.28	0.45	-0.85
-0.15 h_5	0.42	$-\frac{3}{2}$	x	-0.98	0.06	0.19
			y	0.45	-0.80	0.40
			z	0.54	0.42	0.73
0.15 h_6	-0.42	$\frac{3}{2}$	x	-0.98	0.06	-0.19
			y	0.45	-0.80	-0.40
			z	0.28	-0.45	0.85

a -axis and the phase ϕ is not very high.

2. The assumption that the envelope of the helices is circular ($A_j = B_j$) and that all the Cu^{2+} ions have the same moment is supported by the polarimetric data. No significant improvement in the fit was obtained by allowing any of the components of moment to vary.
3. The best agreement (Table II) was achieved for a model comprising two pairs of spins with the A vectors lying in the ab plane ($\theta_A = 90^\circ$) and the B vectors directed along the c axis ($\theta_B = 0^\circ$). The angle between the two planes on which the spin pairs rotate is small, not exceeding 10° . Allowing the 4 helices to be independent did not improve the fit.
4. To check other details of the magnetic structure we need to complement the polarimetric data with the integrated intensity measurements.

The unpolarized integrated intensity sets consist of 98 k^0 magnetic (and 286 nuclear) reflections for the $\text{Cu}_2\text{Te}_2\text{O}_5\text{Cl}_2$ crystal and 44 magnetic (30 nuclear) for the $\text{Cu}_2\text{Te}_2\text{O}_5\text{Br}_2$ crystal. Due to the small size of the $\text{Cu}_2\text{Te}_2\text{O}_5\text{Br}_2$ crystal and its low magnetic moment, very long counting times were needed; measurement of

TABLE III: The k^0 magnetic structure of $\text{Cu}_2\text{Te}_2\text{O}_5\text{X}_2$ ($\text{X}=\text{Cl}, \text{Br}$). The origin of the helices is chosen in the ab plane ($\theta_A = 90^\circ$). The phase of the first helix ϕ_1 is set to 0. $\phi_B = \phi_A + 90^\circ$ due to orthogonality of A_j and B_j . ϕ_B is fixed to zero based on polarization data. ϕ_{ij} ($i, j=1, 4$) is the canting angle between moments of the Cu^{2+} ions with coordinates $x=0.730, y=0.453, z=0.158: 1(x; y; z), 2(1-x; 1-y; z), 3(y; 1-x; z), 4(1-y; x; z)$.

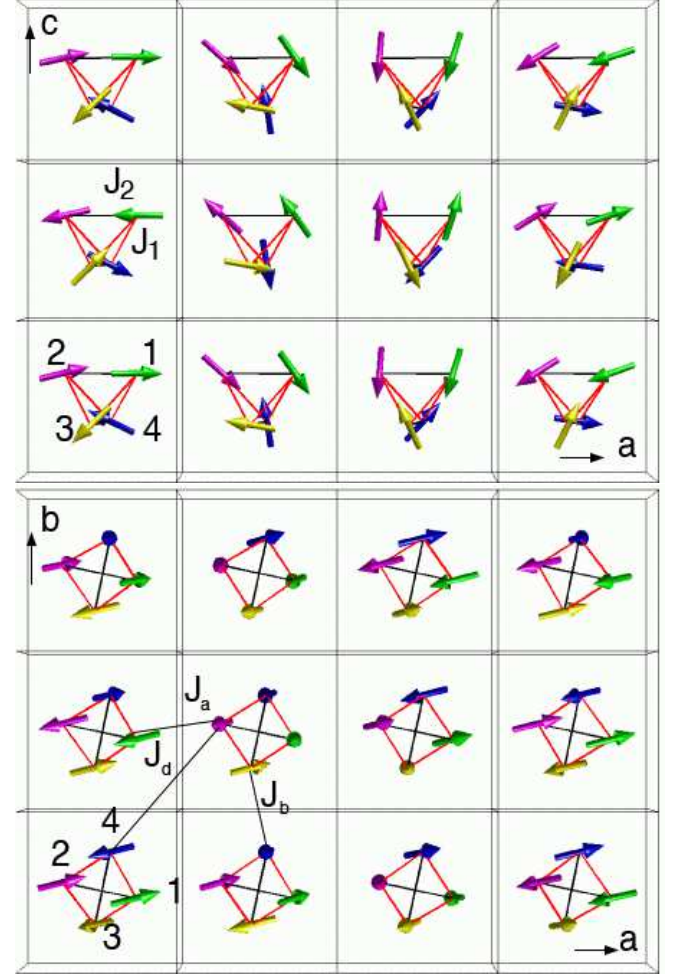
		$m, [\text{B}=\text{Cu}]$	A	2	3	4, [°]
X = Cl		0.88(1)	14(5)	13(3)	44(3)	-26(4)
X = Br		0.395(5)	9(5)	22(4)	75(5)	-46(3)
	12	34	13	14	23	24, [°]
X = Cl	13	70	135	154	147	142
X = Br	22	120	105	134	127	112

each magnetic reflection lasted up to 4.5 h. Nuclear intensities were corrected for absorption and extinction, which for the $\text{Cu}_2\text{Te}_2\text{O}_5\text{Cl}_2$ crystal was significant. When modeling the magnetic structure the scale refined from the nuclear reflections and the parameters reliably determined from the polarimetry experiment were fixed. We assumed a constant moment model and constrained A to lie in the ab plane and B to be parallel to the c axis. The intensity data are sensitive to the absolute values of the magnetic moment and the angles θ_A and ϕ , in contrast to the polarimetric data, and the values obtained from these refinements are given in Table III. The model itself is illustrated schematically in Fig. 2. The goodness of fit of the model in which there was a difference in the θ_A angles of two pairs of 10° was not significantly different from that in which it was zero, so within the statistical accuracy all spins rotate in the same plane.

For $\text{Cu}_2\text{Te}_2\text{O}_5\text{Br}_2$ the same constraints were used in the refinement of the integrated intensity data. The final values are listed in Table III and the structure is presented in Fig. 3. The refinement was much more stable than for the $\text{Cu}_2\text{Te}_2\text{O}_5\text{Cl}_2$ intensity data and always converged to these final values, even when releasing the constraints and starting with different initial values. In fact, a simulated annealing algorithm^{21,22} was applied to the generalised helix model (in which the moments are equal but all other constraints on the helices are relaxed), and the resulting structure was extremely close to that presented in Fig. 3.

The model for the k^0 structure of $\text{Cu}_2\text{Te}_2\text{O}_5\text{Cl}_2$ developed here gives a good fit to the limited k^0 set of reflections measured previously.¹⁴ This model gives very poor agreement with the k reflections, but significant improvement can be achieved by allowing the planes in which the two pairs rotate to be inclined to one another in accordance with the previously determined k model. An interesting detail is that the canting angles ϕ_{12} and ϕ_{34} are almost the same in the k^0 $\text{X}=\text{Cl}, \text{Br}$ and k $\text{X}=\text{Cl}$

FIG. 2: The ac (top) and ab (bottom) view on the layer of spin tetrahedra of the $\text{Cu}_2\text{Te}_2\text{O}_5\text{Cl}_2$ k^0 magnetic structure. The origin is shifted by $[0\ 0\ 1/2]$ relative to the crystallographic unit cell.



structures of $\text{Cu}_2\text{Te}_2\text{O}_5\text{X}_2$.

III. DISCUSSION

The findings of our experiment, namely, the co-existence, in some crystals, of two symmetrically independent wave vectors, k^0 and k ; two different magnetic structures, one associated with each wave vector; two different configurations for the spins in the Cu^{2+} tetrahedra: the 'canted coplanar' and 'canted pair' motifs in these magnetic structures, are very puzzling. The ground state of an isolated tetrahedron with AF exchange interactions between $S=1/2$ spins at the vertices is a singlet: $\sum_{i=1}^4 S_i = 0$. No long range magnetic order would exist in a structure built from such isolated tetrahedra at any temperature. If the tetrahedra have tetragonal rather than cubic symmetry, as in the present case, there are two different intra-tetrahedral exchange

FIG. 3: The ac layer of spin tetrahedra of the $\text{Cu}_2\text{Te}_2\text{O}_5\text{Br}_2$ k^0 magnetic structure.

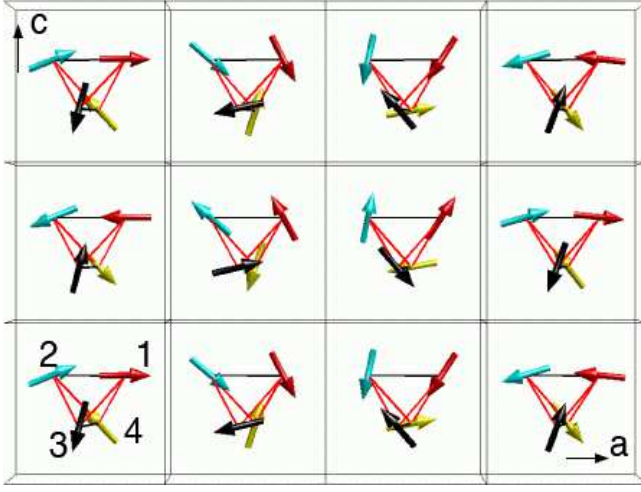


TABLE IV: Comparison between selected observed and calculated magnetic structure factors of k^0 (present D10 experiment, $F^{k^0}; h^{k^0}$) and k (previous D15 experiment, $F^k; h^k$) reflections of $\text{Cu}_2\text{Te}_2\text{O}_5\text{Cl}_2$ crystals.

h^{k^0}	k	l	$F_{\text{obs}}^{k^0}$	$F_{\text{calc}}^{k^0}$	h^k	F_{obs}^k	F_{calc}^k
-0.15	0.42	0.5	7.280	6.487	0.15	8.8130	8.2691
0.15	-0.42	0.5	7.550	6.206	-0.15	8.4691	8.2893
-0.15	-0.58	0.5	8.544	7.545	0.15	7.1362	6.8697
-0.15	-0.58	-0.5	8.602	6.892	0.15	7.2834	6.8684
-0.85	0.58	0.5	8.000	7.426	0.85	2.0599	1.1244
-1.15	0.42	-0.5	5.099	5.118	1.15	2.8397	4.2169
-1.15	-0.58	0.5	5.385	4.851	1.15	3.2573	3.9668
-0.85	-0.42	0.5	3.606	2.003	0.85	5.8267	6.0495
-1.85	-0.42	0.5	5.477	4.607	1.85	7.1667	6.4599
0.15	-0.42	-1.5	8.660	8.310	-0.15	8.8371	7.8371
0.15	-0.42	1.5	8.660	8.285	-0.15	8.5935	7.8208
-0.15	0.42	1.5	8.718	8.310	0.15	8.8130	7.8371
0.15	0.58	-1.5	11.747	12.104	-0.15	5.8990	5.1342
-0.15	-0.58	-1.5	11.874	12.058	0.15	5.9349	5.1453
-0.15	-0.58	1.5	11.662	12.104	0.15	6.4821	5.1342
-0.85	0.58	-1.5	6.000	6.474	0.85	2.0599	0.7765

constants: nearest neighbour J_1 and next nearest neighbour J_2 . If $J_1 > J_2$ the singlet state involves all four spins whereas if $J_1 < J_2$ the spins form two dimers, each dimer individually forming a spin singlet.¹⁰ In the $\text{Cu}_2\text{Te}_2\text{O}_5\text{X}_2$ system due to strong inter-tetrahedral coupling the tetramers and dimers are not true singlets and the ground state is magnetically ordered.

The system is very complex and the ground state spin arrangement is determined by competition between the geometrically frustrated intra-tetrahedral coupling, the exchange between tetrahedra and the antisymmetric Dzyaloshinskii-Moriya interactions. It is possible that the interplay between these various couplings could

result in several different but nearly degenerate spin configurations. In this case the spin system could be prompted to adopt one out of several possible arrangements by perturbations due to oxygen or copper defects associated with slight chemical inhomogeneity. This would explain why the coexistence of k^0 and k is strongly sample dependent. If we consider the lattice defined by the centers of the tetrahedra, ignoring their symmetry, another observation, the equality in the lengths of the components k_x and k_y for the k^0 and k wave vectors, becomes clear. Such a lattice has full tetragonal symmetry and the k^0 and k wave vectors are symmetrically equivalent. This could mean that the length of the wave vector is determined by the inter-tetrahedral exchange and until there is intra-tetrahedral ordering, the two wave vectors are degenerate. We suggest that the final arrangement adopted by the tetrahedra may be determined either by chance nucleation and growth of one rather than the other wave vector or by small alterations in the relative strengths of intra-tetrahedral interactions caused by crystal inhomogeneities.

The k^0 structure is the one which occurs most frequently in the $\text{Cu}_2\text{Te}_2\text{O}_5\text{X}_2$ crystals studied up to now by neutron diffraction. Its main feature is that the helices of all spins rotate almost in a single plane, which is close to (010). The 4 spins of each Cu^{2+} tetrahedron form a canted coplanar motif which rotates on a single helix with propagation vector k^0 . The refined moment is 0.88(1) μ_B/Cu ($\text{X}=\text{Cl}$) and 0.395(5) μ_B/Cu ($\text{X}=\text{Br}$).

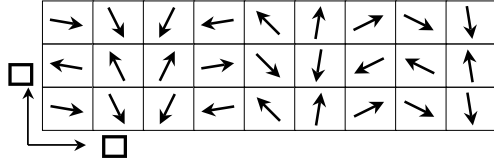
The angles between the spins on the sites 1-2 and 3-4 are very different from one another: the Cu1-Cu2 spins are almost collinear with $\angle_{12} = 13(3)$ ($\text{X}=\text{Cl}$) and $\angle_{12} = 22(4)$ ($\text{X}=\text{Br}$), while the Cu3-Cu4 arrangement is almost orthogonal $\angle_{34} = 70(4)$ ($\text{X}=\text{Cl}$) and $\angle_{34} = 120(5)$ ($\text{X}=\text{Br}$). Noting that the overlap between magnetic orbitals associated with the J_2 path is almost zero^{8,9} this might indicate that the intra-tetrahedral J_2 coupling is rather weak. On the other hand the angles between spins of different pairs in the same tetrahedron differ only slightly (see Table III) and are close to 145 ($\text{X}=\text{Cl}$) and 120 ($\text{X}=\text{Br}$). These angles are the same for all tetrahedra in the structure and such regularity might imply that the J_1 coupling mediated through the Cu-O-Cu superexchange path ($\backslash \text{Cu-O-Cu } 110$) is strong.

Analysis of the angles between spins in adjacent tetrahedra reveals that neighbouring ions across the $[110]$ diagonals are almost antiparallel (Fig. 2 bottom). This implies that the inter-tetrahedral diagonal J_d coupling could be important with the linear superexchange path Cu-X-X-Cu providing a strong AF interaction.^{8,9} The angles between neighbouring ions related by the $[100]$ and $[010]$ lattice translations are very different, in spite of the underlying tetragonal symmetry. One, for $[100]$, is acute ($\sim 40^\circ$) and the other obtuse ($\sim 140^\circ$ $\text{X}=\text{Cl}$, 110° $\text{X}=\text{Br}$) implying weak J_a and J_b coupling in accord with band-structure

calculations.⁸

One further property of the proposed k^0 spin arrange-

FIG. 4: The ac layer of resultant moment of tetrahedra of the $\text{Cu}_2\text{Te}_2\text{O}_5\text{Cl}_2$ k^0 magnetic structure.



ment should be discussed. This model leads to a finite resultant moment on each tetrahedron which is constant throughout the whole crystal. This moment rotates in the ac plane (Fig. 4) on a cycloid with the propagation vector $(k_x, 0, \frac{1}{2})$ giving an angle of 54° ($X=\text{Cl}$) and 62° ($X=\text{Br}$) between the neighbouring tetrahedra along a . Interestingly, the resultant moments on the tetrahedra in the chloride ($0.333 \mu_B$) and bromide ($0.388 \mu_B$) are almost equal, although the moment of

the Cu^{2+} ions is close to the saturated value of $1 \mu_B/\text{Cu}$ for $\text{Cu}_2\text{Te}_2\text{O}_5\text{Cl}_2$, whereas it is significantly less for $\text{Cu}_2\text{Te}_2\text{O}_5\text{Br}_2$.

As the $S=1/2$ Cu^{2+} ion has very little single ion anisotropy, it is not clear what is responsible for the choice of the ac plane as the easy plane of the spins. It might be either the anisotropy of the inter-tetrahedral interactions or the DM interactions the direction of which is determined by the symmetry of the local environment.²³ The DM interaction could be nonzero in the $\text{Cu}_2\text{Te}_2\text{O}_5\text{X}_2$ system and would give a DM vector in the ab plane²⁴ perpendicular to each Cu-Cu bond within the tetrahedra. This antisymmetric coupling would favor two spins to cant in opposite directions in the plane perpendicular to the DM vector and the fairly constant angle between nearest neighbour spins could reflect the ratio DM/J_1 . A thorough theoretical study is needed to clarify a number of questions raised by our findings.

1. What relative strengths of the J_1 , J_2 intra-tetrahedral and J_c , J_d , J_x ²⁰ inter-tetrahedral couplings are needed to give the experimentally observed k^0 and k structures.
2. Can anisotropy of the inter-tetrahedral interactions alone explain the easy plane of the magnetic moments in the k^0 structure.
3. Does the choice of wave vector (k^0 or k) determine the final spin arrangement adopted by the tetrahedra or do changes in strength of the J_1 , J_2 couplings moderate the choice between the k^0 ('canted coplanar') and the k ('canted pair') structures.

Acknowledgments

This work was carried out at the ILL reactor, Grenoble, France and on SINQ at the Paul Scherrer Institute, Villigen, Switzerland. We would like to thank Drs. N. Kemavanois and M. Medarde for experimental assistance during the D3 experiment and Dr. A. M. Mulders for help during the X10 experiment. The sample preparation was supported by the NCCR research pool MAnEP of the Swiss NSF. SJC acknowledges the financial support of the UK Engineering and Physical Sciences Research Council.

* e-mail: Oksana.Zaharko@psich

¹ Magnetic systems with competing interactions, edited by H. T. Diep, World Scientific, Singapore (1994).

² M. Johansson et al., Chem. Mater. 12, 2853 (2000).

³ P. Lemmens, K.-Y. Choi, E. E. Kaul, C. Geibel, K. Becker, W. Brenig, R. Valenti, C. Gros, M. Johansson, P. Millet, and F. Mila, Phys. Rev. Lett. 87, 227201 (2001).

⁴ J. Jensen, P. Lemmens, and C. Gros, Europhys. Lett. 64, 689 (2003).

⁵ C. Gros, P. Lemmens, M. Vojta, R. Valenti, K.-Y. Choi, H. Kageyama, Z. Hiroi, N. V. Mushnikov, T. Goto, M. Johansson, and P. Millet, Phys. Rev. B 67, 174405 (2003).

⁶ M. Prester, A. Smontara, I. Živković, A. Bilušić, D. Drobac, H. Berger, and F. Bussy, Phys. Rev. B 69, 180401

- (2004).
- ⁷ A.V. Sologubenko, R. Dell'Amore, H.R. Ott, and P. Millet, Euro. Phys. Jour. B 42, 549 (2004).
 - ⁸ R. Valenti, T. Saha-Dasgupta, C. Gros, and H. Rosner, Phys. Rev. B 67, 245110 (2003).
 - ⁹ M.-H. Whangbo, H.-J. Koo, and D. Dai, Inorg. Chem 42, 3898 (2003).
 - ¹⁰ W. Brenig, K.W. Becker, Phys. Rev. B 64, 214413 (2001).
 - ¹¹ V.N. Kotov, M.E. Zhitomirsky, M.E. Ilha'jal, F.M. ila, Phys. Rev. B 70, 214401 (2004).
 - ¹² S.J. Crowe, S. Majumdar, M.R. Lees, D.M. K. Paul, D. T. Adroja, S.J. Levett, Phys. Rev. B 71, 224430 (2005).
 - ¹³ O. Zaharko, H.M. Rinnow, A. Daoud-Aldine, S. Streule, F. Junanyi, J. Mesot, H. Berger, and P.J. Brown, Physika Nizkikh Temperatur, 31, 1068 (2005).
 - ¹⁴ O. Zaharko, A. Daoud-Aldine, S. Streule, J. Mesot, P.J. Brown, and H. Berger, Phys. Rev. Lett. 93, 217206 (2004).
 - ¹⁵ Note that in the experiment described in Ref.14 the hkl reflections could not be properly distinguished due to limited access to ϕ -plane reflections on the normal beam geometry D15 diffractometer. The successive experiment on the four-circle geometry TriCS diffractometer revealed that the h and k indices should be reassigned and the determined magnetic arrangement should be denoted k and not k^0 . Symmetry analysis of measured nuclear reflections gave no evidence of growth twins for this crystal possessing two wave vectors k^0 and k below T_N .
 - ¹⁶ M. Blume Phys. Rev. 130, 1670 (1963).
 - ¹⁷ S.V. Maleev, Baryaktar and Suris, Sov. Phys.-Solid State 4, 2533 (1963).
 - ¹⁸ P.J. Brown, J.C. Matthewsman, The Cambridge Crystallography Subroutine Library, 1897.
 - ¹⁹ P.J. Brown, Physica B 297, 198 (2001).
 - ²⁰ Notations from Ref.8 are adopted.
 - ²¹ J. Rodriguez-Carvajal, Physica 192B, 55 (1993).
 - ²² S. Kirkpatrick, C.D. Gelatt Jr., and M.P. Vecchi, Science, 220, 671 (1983).
 - ²³ T. Moria, Phys. Rev. 120, 91 (1960).
 - ²⁴ M.E. Ilha'jal, F.M. ila private communication.